Supplementary Information for "El Niño and health risks from landscape fire emissions in Southeast Asia"

Miriam E. Marlier, Ruth S. DeFries, Apostolos Voulgarakis, Patrick L. Kinney, James T. Randerson, Drew T. Shindell, Yang Chen, and Greg Faluvegi

Model Set-up

GISS-E2-Puccini is the new version of the NASA GISS ModelE general circulation model (http://www.giss.nasa.gov/tools/modelE/). It was run at 2°x2.5° resolution with 40 vertical layers from 1997-2007; we focused on model output that approximately corresponds with the Earth's surface. With our two year spin-up period, we expect any influence of initial conditions on the nonlinear formation of O_3 to be small.

Our simulations included interactive constituents in the PUCCINI model for chemistry, aerosols (sulfate, carbonaceous, nitrate, dust and sea salt), and an aerosol indirect effect parameterization[1,2]. We ran the model without fires and with GFED3 emissions mixed uniformly through the boundary layer. This assumption for the height of smoke injection is justified by previous work by Tosca et al. (2011) with satellite observations of smoke plume heights in Indonesia; 96% of all fire plumes on Sumatra and Borneo were within 500 m of the top of the planetary boundary layer during the morning (10:30 am) MISR overpass[3]. Annually and monthly-varying GFED3 emissions were used for the species available, otherwise we scaled from time-varying CO emissions. Fires do not directly emit the pollutants that we focus on for health effects: $PM_{2.5}$ and O_3. For $PM_{2.5}$, GFED3 emissions contribute black and organic carbon, which can combine with other sources of aerosols (such as sea salt, dust, and sulfate) in our modeled concentrations. GFED3 also contributes O_3 precursors, such as NO_x, CO, and VOC's, which secondarily

produce O_3 in photochemical reactions. Present-day anthropogenic emissions were re-gridded to 2°x2.5° resolution based on Lamarque et al. (2010)[4], which was produced to provide input to models being run in support of the IPCC Fifth Assessment Report (AR5). Methane in the lowest model layer was kept to observed values for each year and lightning NO_x was generated internally based on an updated version of Price et al. (1997)[5]. Isoprene emissions were based on Guenther et al. (1995, 2006)[6,7]; vegetation alkene and paraffin emissions from the GEIA dataset are based on Guenther et al. (1995)[6]. Model winds were linearly relaxed towards reanalysis based on meteorological observations[8].

GEOS-Chem (http://acmg.seas.harvard.edu/geos/index.html) is an off-line atmospheric chemical transport model driven by GEOS-4 meteorological fields from NASA GMAO. We use version v9-01-01 at 2°x2.5° resolution and 30 vertical layers from 1997-2006, with a two year spin-up. Surface values correspond to the middle of the lowest model layer (about 0.06 km, on average). The GEOS-Chem model includes a comprehensive treatment of tropospheric NO_x-hydrocarbon-O_x chemistry, and a simplified treatment of aerosols including black and organic carbon, dust, sea salt, and sulfate-nitrate-ammonium aerosols. Annually and monthly varying fire emissions were scaled from GFED3 carbon emissions and were emitted into the surface layer and mixed throughout. Anthropogenic gas-phase emissions from fossil-fuel use are based on a hybrid of the global GEIA[9,10,11] and EDGAR datasets[12], overwritten by regional datasets for the United States, Canada, Mexico, Europe, and Southeast Asia. Emissions from biofuel combustion are from Yevich and Logan (2003)[13], with regional updates over North America and Southeast Asia. Biogenic emissions from terrestrial vegetation are from the Model of Emissions of Gases and Aerosols from Nature (MEGAN)[7,14,15]. Emissions of SO_2 (non-fossil-fuel combustion) and

NH_3 are as in Park et al (2004)[16]. Other aerosol sources include elemental and organic carbon[17], dust[18], and sea salt[19].

Supplementary Figure S1 is analogous to Figure 2 in the main text, but shows total concentrations and subsequent exceedances in 1997 due to fires and all other sources. The spatial patterns of both $PM_{2.5}$ and O_3 are similar to the fires-only concentrations presented in the main text, indicating the strong influence of fire emissions relative to other sources on total concentrations.

Model Validation

Our model validation comes from three sources: daily visibility observations, annual $PM_{2.5}$, and hourly O_3 measurements (Supplementary Fig. S2). Due to the lack of long-term $PM_{2.5}$ ground monitoring stations in this region, visibility estimates are used to indicate changes in air quality degradation. Daily visibility data are available from the National Climatic Data Center Global Summary of the Day[20]; we then reduced the impact of precipitation and human error on measurements with a monthly filter[21]. Modeled $PM_{2.5}$ includes contributions from biomass burning and all other sources. There were 19 stations located in 13 grid cells; we averaged station data for the 6 grid cells with more than one station. Monthly modeled $PM_{2.5}$ values correlated well with the extinction coefficient derived from visibility measurements. The median R^2 was 0.42-0.67 for GISS-E2-Puccini and GEOS-Chem, with a slightly wider range of correlations for the GISS-E2-Puccini model (Supplementary Table S2). We also averaged Borneo stations and non-Borneo stations and plotted monthly time series comparisons between model estimates and ground observations (Supplementary Fig. S3a). Modeled $PM_{2.5}$ concentrations reproduced the

months with peak fire activity from the extinction coefficient time series, though the relative increases over baseline values in ground observations were better captured by the GISS-E2-Puccini model during the extreme 1997-98 concentrations.

Annual-average $PM_{2.5}$ values for 2005 were recorded at six urban ground stations in Indonesia, Malaysia, Thailand, and Vietnam from a set of observations assembled in support of the Global Burden of Disease Study (GBD 2010, http://www.globalburden.org/index.html) and compared with annual averages from each model (Supplementary Fig. S3b). Each model was generally low compared to station data but with only six stations available only in urban areas, data is too limited to draw firm conclusions. For example, without the single ground station observation of ~50 $\mu g/m^3$, ground observations and model data would become negatively correlated, illustrating the need for a larger set of validation data. We conclude that both models are producing conservative $PM_{2.5}$ concentrations in densely populated areas, consistent with the expectation that values would be higher from stations located in urban areas instead of large model grid boxes.

The World Data Centre for Greenhouse Gases maintains hourly O_3 measurements at two ground stations in our study area (http://gaw.kishou.go.jp/wdcgg/wdcgg.html). The Indonesian station is available from 1/1997-12/2007 and the Malaysian station is available from 9/1997-12/2001 (see Supplementary Fig. S2 for locations). Due to data storage constraints, we saved 1-2pm O_3 data for the GEOS-Chem model, 12-3pm O_3 from the GISS-E2-Puccini model (the finest temporal interval available for output), and 24-hour averages from both models.

For calculating exceedances over WHO air quality guidelines and interim targets (Table S1), we used the 1-2pm concentrations as a proxy for the 8-hour maximum concentrations. Figure S4a shows the strong correlation between 1-2pm O_3 and the 8-hour maximum values, using the hourly values available from ground station data. For calculating O_3-related mortality, we used the 24-hour average concentrations as described in Bell et al. (2005)[22]. We also compared monthly averages of 24-hour O_3 data with reported monthly O_3 station data (with a median of 24 days per month with station data). In the time series comparison, both models reproduce the monthly concentrations seen at the Indonesian site, which was closer to the fire source (Supplementary Fig. S4b). GEOS-Chem was consistently higher at both stations.

$PM_{2.5}$ Scaling Factors

We use satellite observations to help correct for model biases that arise from uncertainties in fire emissions and the representation of aerosol transport in our forward model estimates (Supplementary Fig. S5). While other studies have used satellite AOD to estimate surface-level $PM_{2.5}$[23], we also incorporate differences between fire and non-fire aerosols by calculating separate scaling factors for each source. In our model runs, aerosol components include sulfate, black carbon, organic carbon, sea salt, and dust. Monthly column AOD from each model was first computed from runs with and without GFED3 fire emissions. After re-gridding satellite observations to model resolution, scaling factors for column-integrated fire and non-fire aerosols were calculated separately for the top one-third of our spatial domain that had the highest mean annual levels of AOD, following the approach described in the Supplementary Material of Johnston et al. (2012)[24]. The non-fire

aerosol scaling factor was estimated from the 4 months of the annual cycle with the lowest contribution of fire aerosols to the total aerosol burden (1.02-1.05 for GISS and 1.56-1.96 for GEOS-Chem); the fire aerosol scaling factor was then estimated for the highest 4 months (1.36-1.53 for GISS and 2.01-2.26 for GEOS-Chem; Supplementary Fig. S5).

This method assumes that these areas and time periods are representative of the entire region and time period, although the composition of aerosol sources may differ. In addition, since satellites measure the quantity of aerosols in the atmospheric column, we must develop scaling factors from models based on column estimates. These factors are then applied to modeled surface concentrations that are of interest to population exposure, although the relationship may differ at the surface. We assume that aerosol emissions do not change the vertical profile of the aerosol mass concentration, and therefore the ratio of column AOD to surface aerosol concentration remains constant for a given region during the same season. This assumption may be invalid if the sources of the aerosol particles change substantially, either spatially or temporally. Compared to previous methods using AOD to scale the surface concentration, our approach treats fire and non-fire aerosols separately, which may partly reduce the uncertainty caused by this assumption. The difference between MODIS and MISR AOD also indicates some of the sampling issues with satellite-derived AOD. Satellite observations are made under clear-sky conditions that can be affected by various parameters such as cloud cover, biomass burning, and mineral dust[23], which can cause gaps in AOD observations and bias monthly averages.

Additional Mortality Estimates

In order to provide a plausible range of mortality estimates and to present how sensitive our calculations are to the selected relative risk (RR) equation and choice of cause-specific mortality, we also evaluate the mortality burden due to 1) changes in the shape of the RR equation, 2) additional projected lung cancer deaths, and 3) short-term all-cause mortality summed over each year. These equations and the relationships that we use in the main text are summarized in Supplementary Table S3. We focus on cause-specific baseline mortality rates when possible because they are likely more similar than all-cause rates between developed countries at temperate latitudes (where most large-scale epidemiology studies are conducted) and tropical regions[25].

First, in addition to the power-law relationship that we present in the main text, we compute cardiopulmonary mortality based on logarithmic and linear relationships between RR and exposure to $PM_{2.5}$. These alternative equations have been more widely used but do not account for extreme $PM_{2.5}$ concentrations; the epidemiological studies that they are based on did not have $PM_{2.5}$ observations more than 30 $\mu g/m^3$. For consistency, we recalculated the power-law relationship using baseline cardiopulmonary disease mortality rates (combination of cardiovascular and respiratory diseases)[26].

We first calculated cardiopulmonary mortality based on a log-linear relationship between RR and annual $PM_{2.5}$ concentrations following the approach given in the Environmental Burden of Disease study[25]. This is given by:

(S1) Cardiopulmonary $RR=[(C_{fire}+1)/(C_{nofire}+1)]^{\gamma}$

where γ =0.1551 (0.05624-0.2541)[25] and C_{fire} and C_{nofire} are annual average concentrations from our model results with and without GFED3 emissions. Excess mortality due to fire pollution is then calculated with equations (2) and (3) from the main text.

We then used a linear form of the RR equation, given by:

(S2) Cardiopulmonary RR= $\exp[\delta(C_{fire} - C_{nofire})]$

where δ=0.0128 (0.0077-0.0182)[27], applied only between the observed concentration range in the original epidemiological study of 5.8-30 $\mu g/m^3$. We then used equations (2) and (3) from the main text to calculate attributable cardiopulmonary disease mortality, which was between the log-linear and power-law results (Supplementary Fig. S6a and Table S4).

We also quantify the effect of long-term exposure on lung cancer mortality with three RR estimates. First, we use equations (1) through (3) from the main text with the power-law relationship between risk and $PM_{2.5}$ dose, but with α=0.3195 and β=0.7433 and baseline mortality rates for lung cancer[28]. In addition, we separately calculate lung cancer mortality using the log-linear relationship from equation (S1), but with γ=0.232179 (0.08563-0.37873)[25] and the linear relationship from equation (S2), but with δ=0.0142 (0.0057-0.0234)[27] and truncated between 5.8-30 $\mu g/m^3$. Mortality due to lung cancer was lower than cardiovascular disease; the power-law relationship was generally more conservative than both log-linear and linear RR (Supplementary Fig. S6b and Table S4).

Finally, we calculate the burden of short-term exposure to air pollution on daily all-cause mortality, summed over each year. This helps us to understand how exposure to extreme daily concentrations impacts public health, in addition to specific outcomes from long-term exposure presented above[25]. These all-cause results are not comparable to the

results from Johnston et al. (2012)[24] because this analysis uses daily exposure and corresponding RR only. The RR term is a linear relationship with an upper threshold of 125 $\mu g/m^3$ and follows equation (4) in the main text, but with δ=1% (0.6-1.5%) per 10 $\mu g/m^3$ increase in PM_{10}[25]. We calculate attributable mortality with equations (2) and (5) from the main text. We convert $PM_{2.5}$ to PM_{10} using a ratio of 0.6[25,29] and apply to adults over 30 years, to remain consistent with our other estimates (Supplementary Fig. S6c and Table S4).

Comparison With Previous Estimates

Table S5 presents a summary of the methods used in our health impact analysis and assumptions that were made at each stage, using the best available methodologies. In addition, the following is a comparison of mortality estimates from Southeast Asia attributable to landscape fires in the global analysis of Johnston et al. (2012)[24] and this region-specific paper (refer to Table 1 in Johnston et al. (2012) and Supplementary Table S6). The numbers are not directly comparable because they estimate different mortality burdens for different study regions: all-cause, all-age mortality for the WHO Southeast Asian region[24] versus cause-specific, adults-only mortality for the ASEAN region. However, both studies show a remarkable correspondence in the difference between phases of the ENSO cycle, with approximately a sevenfold increase in mortality during El Niño relative to La Niña. Regardless, the estimates are substantially lower in this paper, largely attributable to the factors described below.

Data for Fire Emissions: Our study presents results from two atmospheric models using GFED3 fire emissions, which were 31% and 17% lower than GFED2 emissions in

Southeast Asia and Equatorial Asia (see Van der Werf et al. (2010) for regional definitions)[30].

Method for Concentration Estimates: We calculate health effects from two baseline models (GISS-E2-Puccini and GEOS-Chem) and four satellite-optimized model datasets, in order to retain a wider plausible range of concentrations. Johnston et al. (2012) merge estimates from GEOS-Chem and two satellite-optimized model datasets. The annual average concentrations reported in Table 1 for GEOS-Chem (baseline model and MISR and MODIS scaled results) are most similar to the Johnston et al. (2012) $PM_{2.5}$ estimates. They are on the lower end of our concentration range, but cannot be directly compared because our estimates also incorporate the reduced regional fire emissions in GFED3.

Concentration-Response Functions (CRF's): We used new power-law relationships between RR and $PM_{2.5}$ concentrations, which were developed only for cardiovascular disease and lung cancer mortality[28]. This relationship is more conservative than using a linear CRF; by explicitly including data from very high concentrations of $PM_{2.5}$ based on studies of exposure to secondhand smoke and cigarette smoke, it avoids extrapolation of linear relationships to high concentrations that can overestimate mortality effects. This accounts for extreme pollutant concentrations that are not observed in ambient air pollution concentrations in the U.S. (which are used to develop epidemiological relationships), but can be experienced in areas close to high fire activity.

Like some previous studies[31], we do not include annual all-cause mortality because of the large differences in underlying conditions that drive baseline all-cause mortality rates between U.S.-based epidemiological studies and our study area. Furthermore, we applied this equation only to the adult population (~40% of the population[32]), instead of to

all ages as in Johnston et al. (2012). The reason is that the power-law function was specifically derived from data for adults.

Our sensitivity analysis with a linear CRF[27] also follows a conservative approach and is not directly comparable to the results from Johnston et al. (2012). We use a new linear CRF estimate and limit the effect between 5.8-30 μg/m^3, which was the concentration range observed in the original epidemiological study. Johnston et al. (2012) used an upper bound threshold of 50 μg/m^3 in the principal analysis.

Region Designation: Our mortality results have different regional definitions than Johnston et al. (2012). The latter global study is separated by 21 WHO subregions; we use a rectangular delineation around ASEAN countries. While these are similar (see Fig. 2 of Johnston et al. (2012) and Fig. 1 in the main text), our study does not include the northern parts of this region, which border China and Bangladesh. The large model grid boxes make it difficult to partition countries within or outside of the study area; these areas have both high concentrations of fire emissions and high populations, so their inclusion will increase mortality estimates in the Johnston et al. (2012) estimates.

Estimate of Annual Mortality: We followed the approach of other modeling studies of pollution health impacts[31,33,25] that use the concept of the attributable fraction to attribute health impacts to a given increase in air pollutant concentrations. Johnston et al. (2012) instead determined whether areas were sporadically or chronically affected by fire, along with a counterfactual level of exposure (theoretical minimum).

Our estimates present 95% confidence intervals around the power-law relationship between RR and mortality. Since the Pope et al. (2011)[28] study did not include confidence

intervals for the reported relationship, we re-calculated the relationship using the upper and lower bounds around the individual RR estimates used in this study.

Additional Health Effects: In addition to annual mortality, we estimate the effect of fire concentrations on other health endpoints by analyzing the spatial distribution of daily exceedances over $PM_{2.5}$ and O_3 concentration thresholds. This is based on annual and 24-hour average $PM_{2.5}$ and 8-hour maximum O_3 concentrations, instead of only using longer-term average model output. Exceedances reference WHO air quality guidelines and interim targets, which combine the results of many epidemiological studies[34].

Supplementary Figures and Tables:

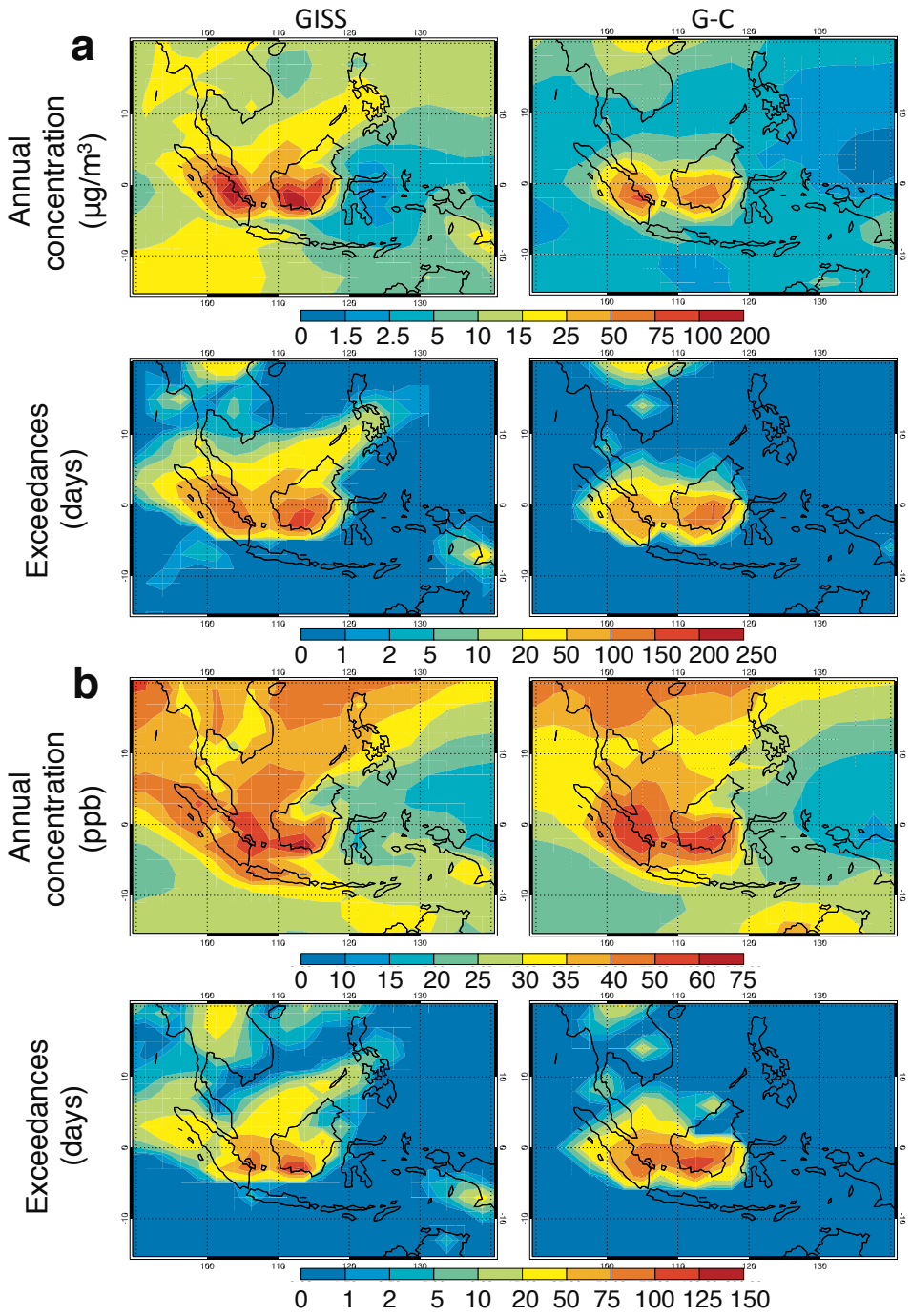

Figure S1. Modeled annual mean 1997 surface concentrations and corresponding daily exceedances in 1997 due to all emissions sources, including fires. a, $PM_{2.5}$ **b**, O_3 annual concentrations due to all sources and daily exceedances over World Health Organization interim targets (50 µg/m^3 daily $PM_{2.5}$ (IT-2) and 80 ppb 8-hour maximum O_3 (IT-1)). Annual concentrations are from 24-hour $PM_{2.5}$ and 8-hour maximum O_3. GISS refers to GISS-E2-PUCCINI and G-C refers to GEOS-Chem.

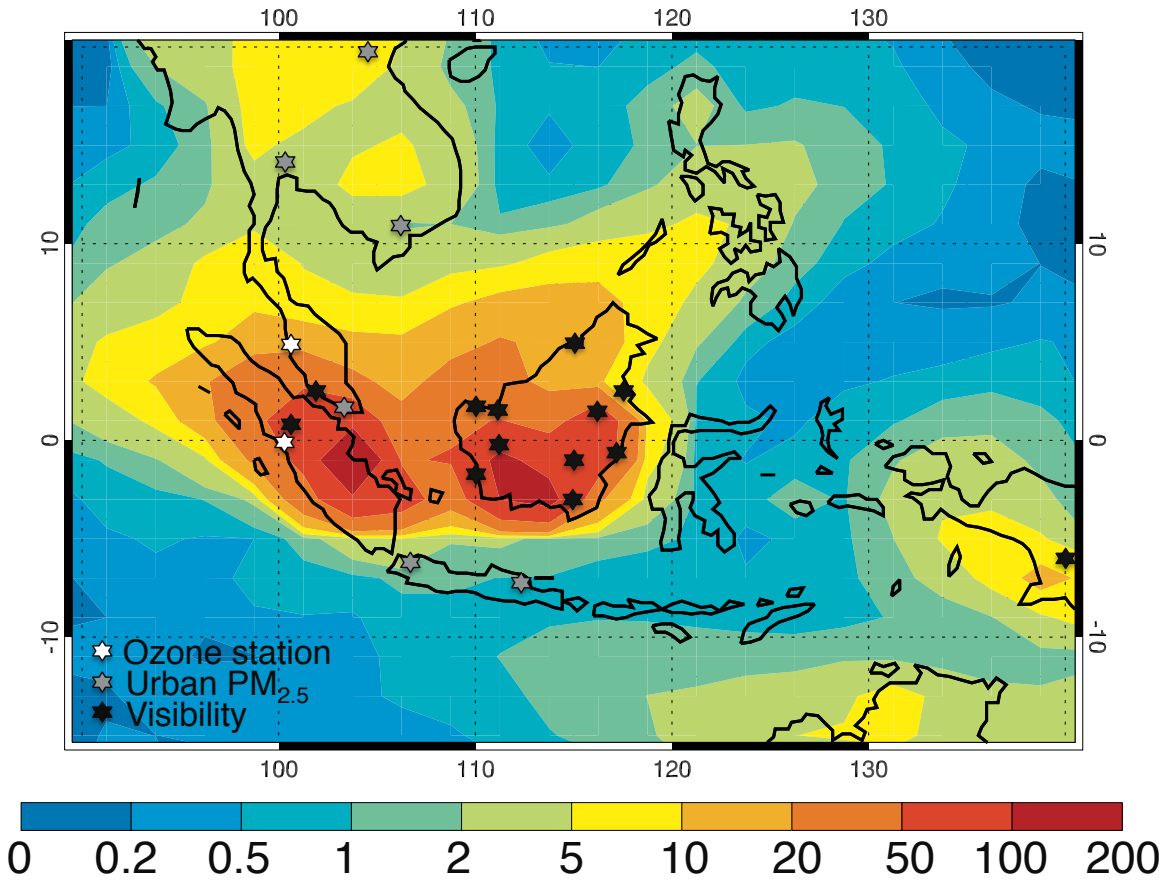

Figure S2. Locations of ground validation data. O_3 stations (white), urban $PM_{2.5}$ stations (gray), and visibility observations (black) are overlaid on the GISS-E2-PUCCINI fires-only 1997 annual average $PM_{2.5}$ concentrations for reference.

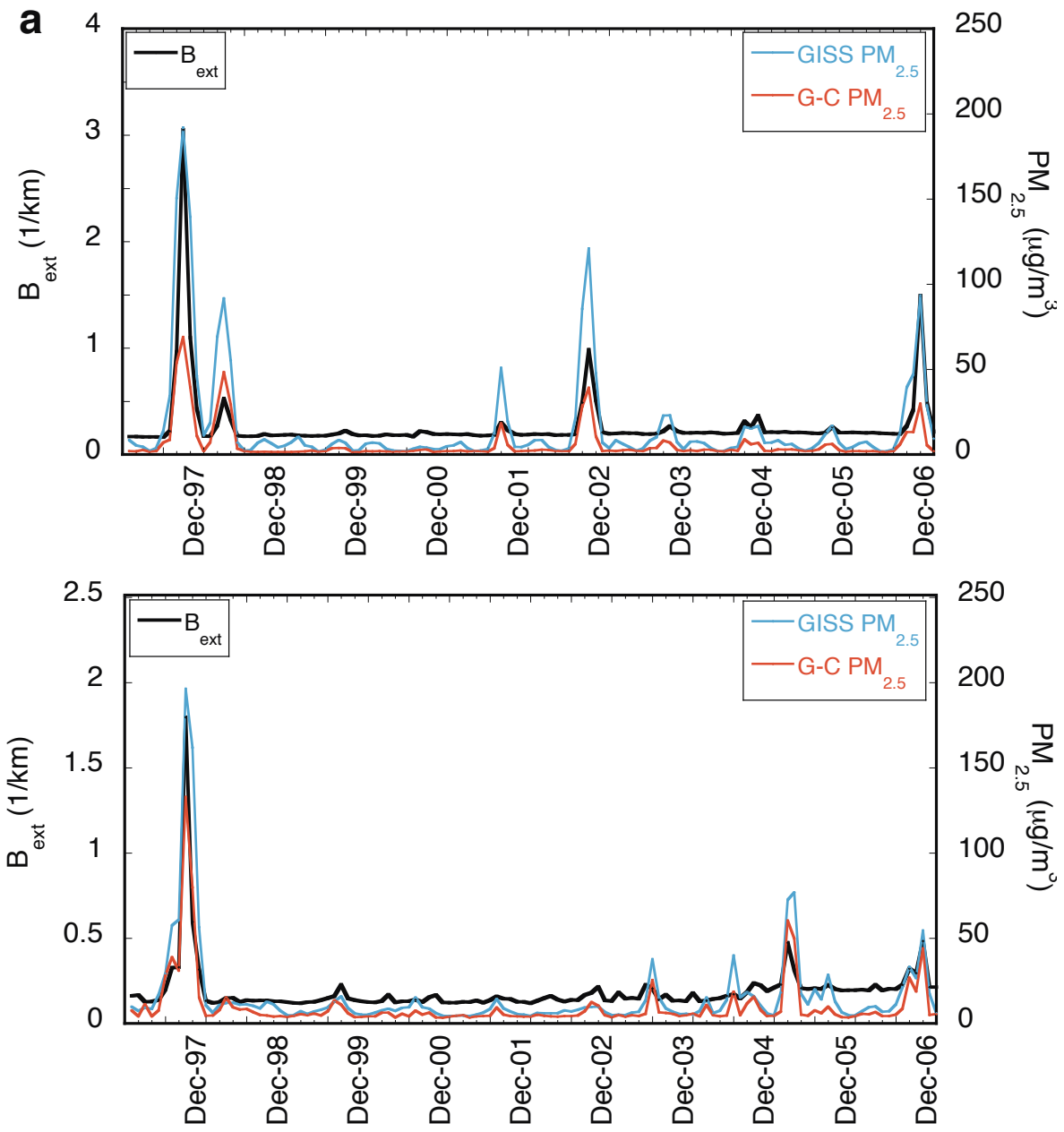
a
B ext
GISS PM 2.5
G-C PM 2.5
B ext (1/km)
PM 2.5 (µg/m3)
0
1
2
3
4
50
100
150
200
250
Dec-97
Dec-98
Dec-99
Dec-00
Dec-01
Dec-02
Dec-03
Dec-04
Dec-05
Dec-06
0
0.5
1
1.5
2
2.5

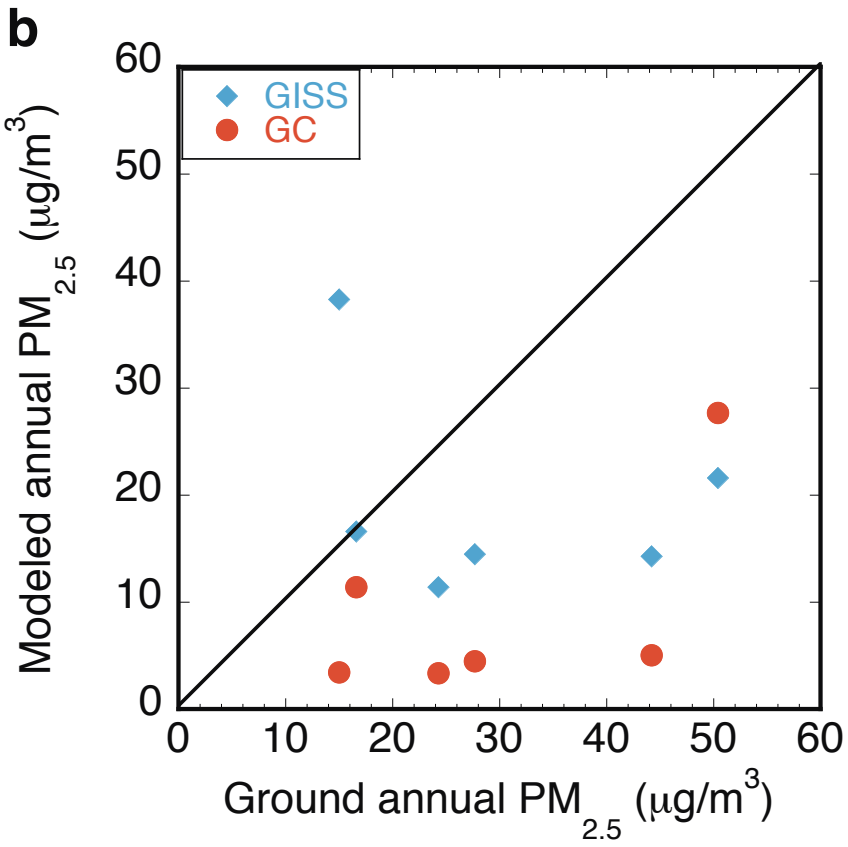

Figure S3. Modeled $PM_{2.5}$ comparison with monthly visibility observations and annual urban $PM_{2.5}$ stations. a, Monthly time series of the observed visibility extinction coefficient (in km^{-1}) and modeled $PM_{2.5}$ for Borneo stations (top) and non-Borneo stations (bottom). Ground observations from the National Climatic Data Center[20]. **b**, 2005 annual $PM_{2.5}$ urban station measurements and annual modeled $PM_{2.5}$ results. Station data from the Global Burden of Disease study (GBD 2010, http://www.globalburden.org/index.html). Satellite-scaled estimates not shown.

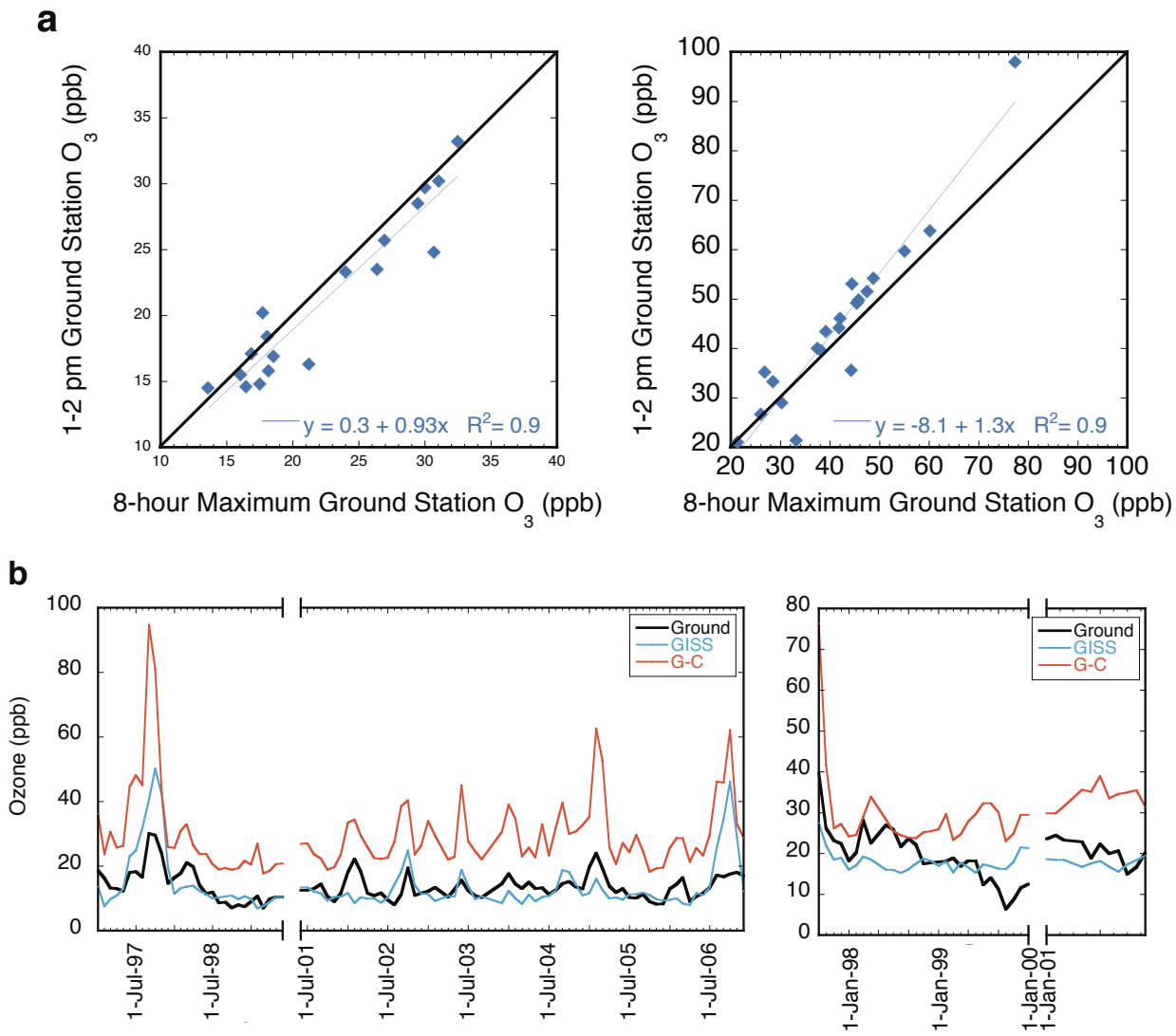

Figure S4. Modeled O_3 comparison with ground station observations. a, Comparison between 1-2pm and 8-hour maximum O_3 for January (left) and October (right) 1997 at the Bukit, Indonesia ground station. Strong correlation supports our use of modeled 1-2pm values as a proxy for the 8-hour maximum, which is needed for WHO exceedance calculations. **b,** Monthly average ground station and modeled O_3 for 1997-2006 in Bukit, Indonesia (left) and 1997-1999 Tanah Rata, Malaysia (right). Ground station data are from World Data Center for Greenhouse Gases (http://gaw.kishou.go.jp/wdcgg/wdcgg.html). GISS refers to GISS-E2-PUCCINI and G-C refers to GEOS-Chem.

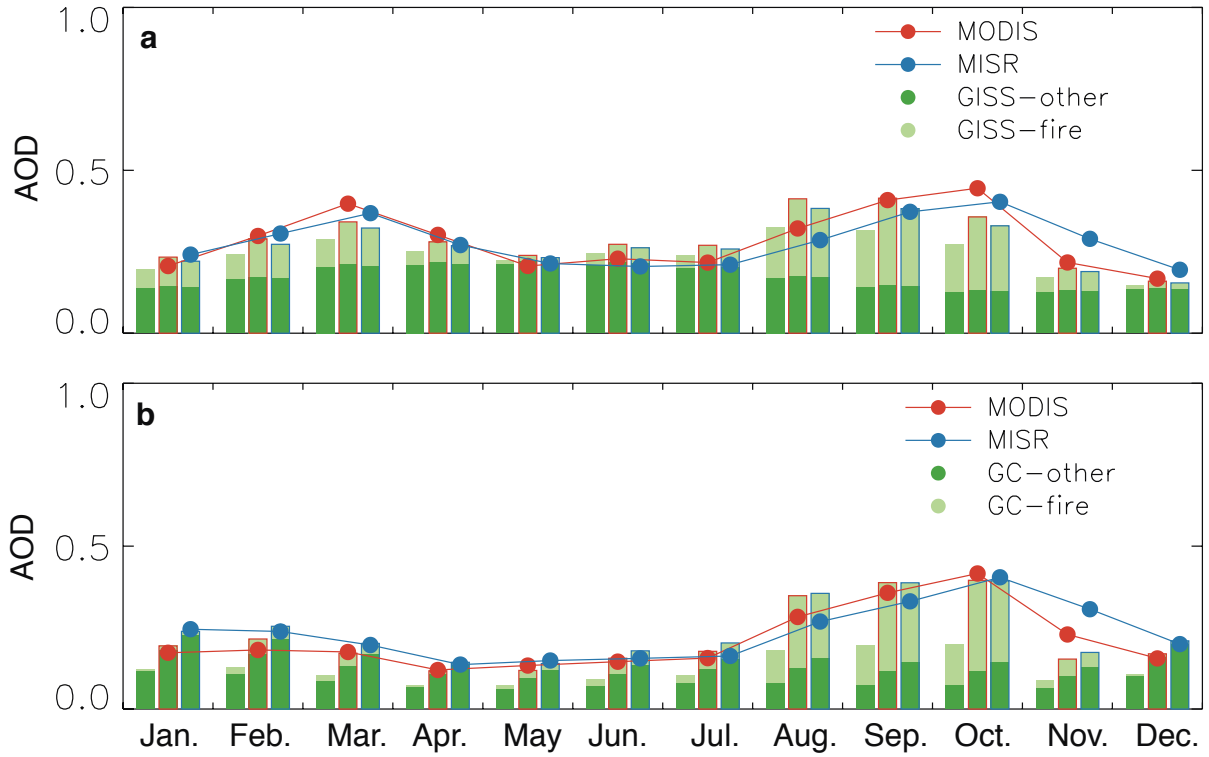

Figure S5. 2001-2006 monthly mean modeled AOD from fires and other sources for the top fire-affected area. a, GISS-E2-PUCCINI (GISS) results. **b**, GEOS-Chem (GC) results. First bar shows baseline model results without scaling factors and second and third bars, respectively, show model results after applying MODIS and MISR satellite constraints. Lines correspond to original MODIS and MISR AOD for reference.

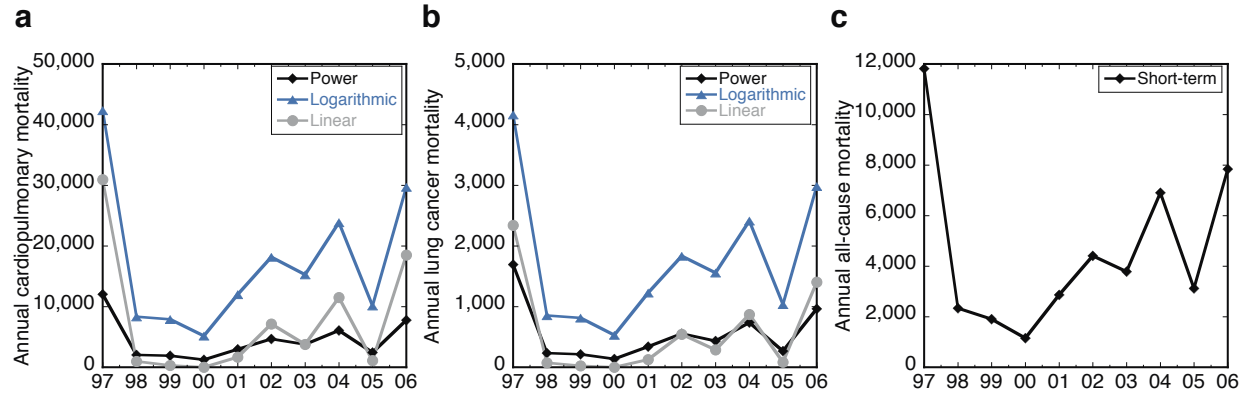

Figure S6. Sensitivity analysis of modeled annual mortality from fires-only $PM_{2.5}$ exposure. a,b, Cardiopulmonary disease (CPD) and lung cancer (LC) mortality from power, logarithmic, and linear relative risk equations. **c**, Annual sum of all-cause mortality from daily exposure. Results are from GISS-E2-PUCCINI only, which was a mid-range concentration estimate.

Table S1. World Health Organization (WHO) $PM_{2.5}$ and O_3 air quality guidelines (AQGs, in bold) and higher interim target (IT) concentration levels. The WHO uses IT levels to summarize expected health risks for countries that cannot immediately achieve AQGs. Note that these guidelines are published by the WHO to assist policymakers in developing standards, but there is no clear evidence for thresholds below which no impacts can be expected[34].

	Level	Averaging Time	Effects
$PM_{2.5}$	**25 µg/m³**	**24-hour**	**Air Quality Guideline (AQG)**
	37.5 µg/m³	24-hour	IT-3: 1.2% increase in short-term mortality over AQG
	50 µg/m³	24-hour	IT-2: 2.5% increase in short-term mortality over AQG
	75 µg/m³	24-hour	IT-1: 5% increase in short-term mortality over AQG
$PM_{2.5}$	**10 µg/m³**	**Annual**	**AQG**
	15 µg/m³	Annual	IT-3: Reduces mortality risk 6% over 25 µg/m³ IT-2.
	25 µg/m³	Annual	IT-2: Reduces mortality risk 6% over 35 µg/m³ IT-1
	35 µg/m³	Annual	IT-1: 15% long-term mortality risk increase over AQG
O_3*	**100 µg/m³***	**Max. daily 8-hour**	**AQG**
	160 µg/m³	Max. daily 8-hour	IT-1: 3-5% increase in mortality over AQG
	240 µg/m³	Max. daily 8-hour	High levels: 5-9% increase in mortality over AQG

*O_3 concentration: 50 ppb ≈ 100 µg/m³.

Table S2. R^2 values for monthly GISS-E2-PUCCINI and GEOS-Chem $PM_{2.5}$ with the monthly extinction coefficient from visibility observations. Results are presented for stations located in Borneo and other sites in the region, refer to Supplementary Figure S2 for specific locations.

	Location (°)	GISS	G-C
Non-Borneo	2.27, 102.25	0.66	0.63
	-6.08, 141.18	0.40	0.16
	0.47, 101.45	0.42	0.84
	Median	**0.42**	**0.63**
Borneo	1.22, 111.45	0.76	0.39
	4.93, 114.93	0.43	0.65
	1.48, 110.33	0.66	0.78
	2.12, 117.45	0.43	0.37
	-0.35, 111.78	0.75	0.71
	-0.95, 114.90	0.79	0.57
	-0.62, 117.15	0.11	0.14
	-1.85, 109.97	0.84	0.82
	-1.27, 116.90	0.19	0.20
	-3.43, 114.75	0.67	0.72
	Median	**0.67**	**0.61**

Table S3. Summary of the equations used to estimate mortality due to $PM_{2.5}$ exposure. Abbreviations are defined in main text and Supplementary Information.

Equation	Details	Source
Cardiovascular RR= $1+ \alpha(I*C)^{\beta}$	Equation developed for use over wide $PM_{2.5}$ dose range; apply to fire and no-fire runs separately to account for nonlinearity	Pope et al. (2011)
Cardiopulmonary RR= $[(C_{fire}+1)/(C_{nofire}+1)]^{\gamma}$	Log-linear relationship between RR and $PM_{2.5}$ exposure decreases risk at high concentrations relative to linear relationship	Ostro et al. (2004)
Cardiopulmonary RR= $\exp[\delta(C_{fire} - C_{nofire})]$	Truncated linear effect between observed concentrations in original study	Krewski et al. (2009)
Lung Cancer Mortality	Estimates an additional long-term cause-specific health impact due to $PM_{2.5}$ exposure	See above studies
All-Cause RR= $\exp[\delta(C_{fire} - C_{nofire})]$	Estimates short-term health impacts; daily $PM_{2.5}$ exposure relationship was developed for all-cause mortality	Ostro et al. (2004)

Table S4. Fires-only mortality using different $PM_{2.5}$ estimates for a strong El Niño year (1997) and La Niña year (2000). Total ASEAN cardiopulmonary disease (CPD) and lung cancer (LC) mortality due to fires only ($x10^3$ people), calculated from three separate equations (see Supplementary Table S3) with the range from 95% confidence intervals. GISS refers to GISS-E2-PUCCINI and G-C refers GEOS-Chem, both also with MISR and MODIS satellite scaling factors.

		Mortality ($x10^3$ people)			
		1997		*2000*	
		CPD	*LC*	*CPD*	*LC*
GISS	*Power*	12.1 (9.7-14.0)	1.7 (1.3-2.1)	1.2 (1.0-1.5)	0.1 (0.1-0.2)
	Log-linear	42.3 (16.5-64.8)	4.2 (1.7-6.2)	5.2 (1.9-8.4)	0.5 (0.2-0.9)
	Linear	30.9 (19.8-41.3)	2.3 (1.0-3.5)	0.0 (0.0-0.0)	0.0 (0.0-0.0)
G-C	*Power*	10.6 (8.3-13.1)	1.1 (0.8-1.5)	1.8 (1.4-2.3)	0.1 (0.1-0.2)
	Log-linear	41.2 (15.7-64.2)	4.1 (1.6-6.3)	7.8 (2.9-12.7)	0.8 (0.3-1.3)
	Linear	17.6 (11.2-23.6)	1.3 (0.6-2.0)	0.0 (0.0-0.0)	0.0 (0.0-0.0)
GISS MISR	*Power*	14.4 (11.7-16.5)	2.1 (1.7-2.6)	1.6 (1.3-2.0)	0.2 (0.1-0.2)
	Log-linear	49.4 (19.4-75.3)	4.8 (2.0-7.2)	6.8 (2.5-11.0)	0.7 (0.3-1.1)
	Linear	36.3 (23.2-48.6)	2.7 (1.2-4.1)	0.0 (0.0-0.0)	0.0 (0.0-0.0)
G-C MISR	*Power*	12.3 (9.9-14.4)	1.7 (1.3-2.1)	2.1 (1.7-2.6)	0.2 (0.2-0.3)
	Log-linear	45.1 (17.3-70.2)	4.5 (1.8-6.8)	8.9 (3.3-14.5)	0.9 (0.3-1.5)
	Linear	28.0 (17.9-37.6)	2.1 (0.9-3.2)	0.0 (0.0-0.0)	0.0 (0.0-0.0)
GISS MODIS	*Power*	15.2 (12.4-17.4)	2.3 (1.8-2.8)	1.8 (1.4-2.1)	0.2 (0.2-0.3)
	Log-linear	51.8 (20.3-79.0)	5.1 (2.1-7.5)	7.3 (2.7-11.9)	0.8 (0.3-1.2)
	Linear	40.5 (25.7-54.3)	3.1 (1.3-4.6)	0.0 (0.0-0.0)	0.0 (0.0-0.0)
G-C MODIS	*Power*	14.8 (11.8-17.5)	1.9 (1.5-2.4)	2.8 (2.2-3.4)	0.3 (0.2-0.4)
	Log-linear	54.4 (21.0-84.3)	5.4 (2.2-8.2)	11.9 (4.3-19.3)	1.2 (0.5-2.0)
	Linear	32.6 (20.7-43.8)	2.5 (1.1-3.7)	0.0 (0.0-0.0)	0.0 (0.0-0.0)
AVERAGE	***Power****	**13.2 (8.3-17.5)**	**1.8 (0.8-2.8)**	**1.9 (1.0-3.4)**	**0.2 (0.1-0.4)**
	Log-linear*	**47.4 (15.7-79.0)**	**4.7 (1.6-8.2)**	**8.0 (1.9-19.3)**	**0.8 (0.2-2.0)**
	Linear*	**31.0 (11.2-54.3)**	**2.3 (0.6-4.6)**	0.0 (0.0-0.0)	0.0 (0.0-0.0)

*Maximum error range.

Table S5. Summary of each stage of methods, the assumptions that were made, and the probable influence on our health impact estimates.

Method	Assumption	Direction of Uncertainty
Fire Emissions	Burned area detects most fires in the region	Uncertain; perhaps underestimate because missing small fires
Model structure	Large grid boxes representative of exposure	Mixed: possible underestimate in urban areas, overestimate in rural areas
Model concentration	Model accurately simulates surface concentrations	Potential underestimate: satellite AOD and ground $PM_{2.5}$ observations higher than model
PM Toxicity	Toxicity of fire $PM_{2.5}$ is similar to urban $PM_{2.5}$ from epidemiological studies	Uncertain: data is too limited on toxicity differences to use a specific biomass burning smoke equation
WHO guidelines	Concentration levels indicative of health effects	Underestimate: health effects likely occur below guideline levels
Cause-specific mortality	Focusing on diseases with direct impacts of fire emissions	Underestimate: impacts multiple additional health conditions
Adults-only mortality	Epidemiological equations were developed for adults, cannot apply to entire population	Underestimate: population under 30 years is a large fraction of population and infants and children are highly susceptible to air pollution
Concentration-response function	Power-law function is the best representation of mortality response	Possible underestimate: power-law function reduced mortality estimates compared with linear or log-linear functions

Table S6. Comparison of mortality estimation approach used by Johnston et al. (2012) and this study. Highlights the different components used to calculate the mortality burden for the Southeast Asian estimates given in the global analysis[24] and our results.

	Johnston et al. (2012)	**This paper**
Data for fire emissions	GFED2	GFED3
Method for concentration estimates	Merge GEOS-Chem model with two satellite AOD optimized results	Separate GISS and GEOS-Chem models, each with additional satellite AOD optimized results
Concentration-response function	Linear for all ages	Power law for adults only
Mortality included	All-cause (A-C)	Cardiovascular (CVD); Lung cancer (LC)
Region designation	WHO subregion	Rectangular area including ASEAN countries
Estimate of annual mortality	El Niño*: 296,000 A-C La Niña*: 43,000 A-C	El Niño**: 10,800 (6,800-14,300) CVD 1,800 (800-2,800) LC La Niña**: 1,600 (800-2,800) CVD 200 (0-800) LC

*September to August; **July to June

Supplementary References

1. Shindell, D. T. *et al.* Simulations of preindustrial, present-day, and 2100 conditions in the NASA GISS composition and climate model G-PUCCINI. *Atmos. Chem. Phys.* **6**, 4427–4459 (2006).
2. Koch, D., Schmidt, G. A. & Field, C. V. Sulfur, sea salt, and radionuclide aerosols in GISS ModelE. *J. Geophys. Res.* **111**, D06206 (2006).
3. Tosca, M. G. *et al.* Dynamics of fire plumes and smoke clouds associated with peat and deforestation fires in Indonesia. *J. Geophys. Res.* **116**, D08207 (2011).
4. Lamarque, J.-F. *et al.* Historical (1850–2000) gridded anthropogenic and biomass burning emissions of reactive gases and aerosols: methodology and application. *Atmos. Chem. Phys.* **10**, 7017–7039 (2010).
5. Price, C., Penner, J. & Prather, M. NO_x from lightning 1. Global distribution based on lightning physics. *J. Geophys. Res.* **102**, 5929–5941 (1997).
6. Guenther, A. *et al.* A global model of natural volatile organic compound emissions. *J. Geophys. Res.* **100**, 8873–8892 (1995).
7. Guenther, A. *et al.* Estimates of global terrestrial isoprene emissions using MEGAN (Model of Emissions of Gases and Aerosols from Nature). *Atmos. Chem. Phys.* **6**, 3181–3210 (2006).
8. Rienecker, M. M. *et al.* MERRA: NASA's Modern-Era Retrospective Analysis for Research and Applications. *J. Climate* **24**, 3624–3648 (2011).
9. Benkovitz, C. M. *et al.* Global gridded inventories of anthropogenic emissions of sulfur and nitrogen. *J. Geophys. Res.* 29239–29253 (1996).
10. Piccot, S. D., Watson, J. J. & Jones, J. W. A global inventory of volatile organic compound emissions from anthropogenic sources. *J. Geophys. Res.* **97**, 9897–9912 (1992).
11. Wang, Y., Jacob, D. J. & Logan, J. A. Global simulation of tropospheric O3-NO x-hydrocarbon chemistry 1. Model formulation. *J. Geophys. Res.* **103**, 10713–10725 (1998).
12. Olivier, J. G. J. & Berdowski, J. J. M. Global emissions sources and sinks. *The Climate System* 33–78 (2001).
13. Yevich, R. & Logan, J. A. An assessment of biofuel use and burning of agricultural waste in the developing world. *Global Biogeochem. Cycles* **17**, 1095 (2003).
14. Sakulyanontvittaya, T. *et al.* Monoterpene and sesquiterpene emission estimates for the United States. *Environ. Sci. Technol.* **42**, 1623–1629 (2008).
15. Guenther, A. & Wiedinmyer, C. *User's guide to the Model of Emissions of Gases and Aerosols from Nature (MEGAN)*. (2007).
16. Park, R. J., Jacob, D. J., Field, B. D., Yantosca, R. M. & Chin, M. Natural and transboundary pollution influences on sulfate-nitrate-ammonium aerosols in the United States: implications for policy. *J. Geophys. Res.* **109**, D15204 (2004).
17. Bond, T. C. *et al.* Historical emissions of black and organic carbon aerosol from energy-related combustion, 1850–2000. *Global Biogeochem. Cycles* **21**, GB2018 (2007).
18. Fairlie, T. D., Jacob, D. J. & Park, R. J. The impact of transpacific transport of mineral dust in the United States. *Atmos. Environ.* **41**, 1251–1266 (2007).
19. Alexander, B. *et al.* Sulfate formation in sea-salt aerosols: constraints from oxygen

isotopes. *J. Geophys. Res.* **110**, D10307 (2005).
20. *Global Surface Summary of Day*. (National Climatic Data Center: Asheville, 2010).at <http://www.ncdc.noaa.gov/cgi-bin/res40.pl?page=gsod.html>
21. Husar, R. B., Husar, J. D. & Martin, L. Distribution of continental surface aerosol extinction based on visual range data. *Atmos. Env.* **34**, 5067–5078 (2000).
22. Bell, M. L., Dominici, F. & Samet, J. M. A meta-analysis of time-series studies of ozone and mortality with comparison to the National Morbidity, Mortality, and Air Pollution Study. *Epidemiology* **16**, 436–445 (2005).
23. Van Donkelaar, A. *et al.* Global estimates of ambient fine particulate matter concentrations from satellite-based aerosol optical depth: development and application. *Environ. Health Perspect.* **118**, 847–855 (2010).
24. Johnston, F. H. *et al.* Estimated Global Mortality Attributable to Smoke from Landscape Fires. *Environ. Health Perspect.* **120**, 695–701 (2012).
25. Ostro, B. *Outdoor air pollution: assessing the environmental burden of disease at national and local levels*. WHO Environmental Burden of Disease Series, No. 5 (World Health Organization: Geneva, 2004).
26. World Health Organization, Department of Measurement and Health Information *Death estimates for 2008 by cause for WHO Member States*. (2011).at <http://www.who.int/healthinfo/global_burden_disease/estimates_country/en/index.html>
27. Krewski, D. *et al. Extended follow-up and spatial analysis of the American Cancer Society study linking particulate air pollution and mortality. HEI Research Report, 140*. (Health Effects Institute: Boston, 2009).
28. Pope, C. A. *et al.* Lung cancer and cardiovascular disease mortality associated with ambient air pollution and cigarette smoke: shape of the exposure-response relationships. *Environ. Health Perspect.* **119**, 1616–1621 (2011).
29. Cohen, A. J. *et al.* Urban air pollution. *Comparative Quantification of Health Impacts: Global and Regional burden of Disease Due to Selected Major Risk Factors* 1353–1434 (2004).
30. van der Werf, G. R. *et al.* Global fire emissions and the contribution of deforestation, savanna, forest, agricultural, and peat fires (1997–2009). *Atmos. Chem. Phys.* **10**, 11707–11735 (2010).
31. Anenberg, S. C., Horowitz, L. W., Tong, D. Q. & West, J. J. An estimate of the global burden of anthropogenic ozone and fine particulate matter on premature human mortality using atmospheric modeling. *Environ. Health Persp.* **118**, 1189–1195 (2010).
32. *World Population Prospects: The 2010 Revision, CD-ROM Edition.* (United Nations, Department of Economic and Social Affairs Population Division: 2011).
33. Schmidt, A. *et al.* Excess mortality in Europe following a future Laki-style Icelandic eruption. *Proc. Natl. Acad. Sci. USA* **108**, 15710–15715 (2011).
34. *WHO air quality guidelines for particulate matter, ozone, nitrogen dioxide and sulfur dioxide*. (World Health Organization: Geneva, 2006).